Chapter 5
Circulating Tumor Cells as Predictive Marker in Metastatic Disease

Mazen A. Juratli, Dmitry A. Nedosekin, Mustafa Sarimollaoglu, Eric R. Siegel, Ekaterina I. Galanzha, and Vladimir P. Zharov

Abstract Numerous studies have demonstrated that circulating tumor cell (CTC) number in peripheral blood correlates with therapy efficiency in various tumors, and can serve as a prognostic marker of metastasis development. Recent clinical data support many oncologists' opinion that some medical procedures may provoke metastasis by triggering increased tumor cell shedding into circulation, but no systematic study has been performed. The development of an *in vivo* flow cytometry method for real-time CTC quantification can provide insights on CTC release dynamics during different medical interventions and possibly long and short term outcome predictions.

Noninvasive enumeration of CTCs is the most direct way to confirm the central hypothesis that tumor manipulations during medical interventions can promote liberation of CTC into the bloodstream. Incisional biopsy and complete tumor resection in melanoma-bearing mice were conducted and the CTC rate was monitored before, during, and for a short-term after the procedures. Incisional biopsy significantly increased CTC counts (up to 60-fold), whereas complete tumor resection significantly decreased CTC counts. Long-term *in vivo* monitoring of CTC triggered by punch biopsy and complete tumor resection was performed on breast cancer- bearing mice. After punch biopsy, the number of CTC increased. In contrast, complete tumor resection significantly decreased the CTC count. New techniques were proposed for labeling newly released CTCs in order to identify them among previously circulating cells.

M.A. Juratli (✉)
Department of General and Visceral Surgery, Goethe-University Hospital of Frankfurt, Frankfurt am Main, Germany

Winthrop P. Rockefeller Cancer Institute, Arkansas Nanomedicine Center, University of Arkansas for Medical Sciences (UAMS), 4301 West Markham, Little Rock, AR 72205, USA
e-mail: Mazen.Juratli@kgu.de

D.A. Nedosekin • M. Sarimollaoglu • E.R. Siegel • E.I. Galanzha • V.P. Zharov
Winthrop P. Rockefeller Cancer Institute, Arkansas Nanomedicine Center, University of Arkansas for Medical Sciences (UAMS), 4301 West Markham, Little Rock, AR 72205, USA
e-mail: DNedosekin@uams.edu; MSarimollaoglu@uams.edu; SiegelEricR@uams.edu; EGalanzha@uams.edu; ZharovVladimirP@uams.edu

M.W. Retsky, R. Demicheli (eds.), *Perioperative Inflammation as Triggering Origin of Metastasis Development*, DOI 10.1007/978-3-319-57943-6_5

These findings have broad clinical implications to reduce viable CTCs release during diagnostics and treatments by real-time monitoring of CTC dynamics followed by well-timed treatment to reduce CTCs in the blood.

Keywords Circulating tumor cell • Melanoma • Breast cancer • Surgery • Biopsy • *In vivo* flow cytometry

5.1 Circulating Tumor Cells (CTCs)

Up to 90% of cancer deaths are related to metastasis in distant organs due to the hematogenous and lymphatics dissemination of circulating tumor cells (CTCs) shed from the primary tumor [1–5]. Despite major effort, challenges remain in treating advanced stages of disease in patients in whom distant metastases develop [1–3]. It would be extremely helpful to have an ultrasensitive blood cancer test (liquid biopsy) for early stages of metastatic diseases, when well-timed therapy is more effective. CTCs at early disease stages are present in the bloodstream in extremely low concentrations: ≤10 CTC/mL. The invasion of tumor cells in the circulation may occur very early in tumor development, thus emphasizing the potential importance of sensitive detection of CTCs and circulating tumor microemboli (CTM).

5.2 Cancer Treatment and CTC Release

A growing body of clinical data suggests that medical diagnostic and therapeutic procedures such as surgery, chemotherapy and radiation therapy may trigger tumor cell shedding into the circulation and thus increase the risk of metastasis. However, data on CTC release due to medical interventions such as tumor palpation, biopsy, or surgery is controversial [6–10]. Some previous studies have shown an increase in CTC number using *in vitro* methods after surgical tumor resection [9], while others observed a decrease in CTC count after surgery or metastases resection [10, 11]. Wind et al. [12] reported significantly fewer CTC during laparoscopic surgery compared to open surgery in patients with colon cancer during tumor resection. The major drawback of these studies is that CTC enumeration is performed several hours after tumor resection, and likely could miss the transient increase in CTC number during or immediately after surgery because of the short CTC lifetime (0.5–4 h depending on CTC metastatic activity) [13–16]. Moreover, the effective difference between surgical invasiveness of cancer such as incisional biopsy and excisional biopsy in term of CTC release into the blood stream is suggested to play an important role in tumor diagnosis and treatment. Incisional biopsy could result in increased risk of metastasis by increasing the CTC count [8, 17]. This effect was observed both using an *ex vivo* model and after the biopsy.

Real-time *in vivo* fluorescence imaging was used to reveal an increase in CTC count in lymphatic vessels after applying 25 or 250 g of pressure for 10 s on the tumor, but no dynamics studies were performed and no correlation with metastasis progression has been established [18]. Unfortunately, this and most other previous studies have not reported crucial tumor manipulation details (e.g. palpation, compression, or partial resection) or lack a comprehensive comparison of the outcomes for different manipulations.

5.3 Principles of *In Vivo* Flow Cytometry with Photoacoustic and Fluorescence Detection Techniques

In vivo flow cytometry (FC), which was invented in 2004, can quantitatively monitor circulating cells *in vivo*, both noninvasively and dynamically [19–28]. Pigmented and fluorescent cells can be detected *in vivo* using dual-contrast photoacoustic (PA) fluorescence flow cytometry (PAFFC) [22]. The method uses laser irradiation of peripheral blood vessels to induce acoustic waves (PA effect) from pigmented cells (e.g., melanoma with intrinsic melanin as PA contrast agent) or fluorescence from cells containing fluorescent proteins (e.g. green fluorescent protein, GFP) in blood flow. The transient increase in blood PA background caused by the presence of a pigmented cell is detected by an ultrasound transducer attached to the skin. The photomultiplier tube detects transient increase in fluorescence from vessels [29–31]. The PA background is associated with the absorption of randomly distributed red blood cells (RBCs) in the irradiated volume, whereas the fluorescence background is related to the autofluorescence from blood and plasma components. In fluorescence flow cytometry (FFC), a cell emits fluorescence photons under continuous wave (CW) laser excitation, whereas PA flow cytometry (PAFC) uses nanosecond pulse lasers to generate PA signals (Fig. 5.1).

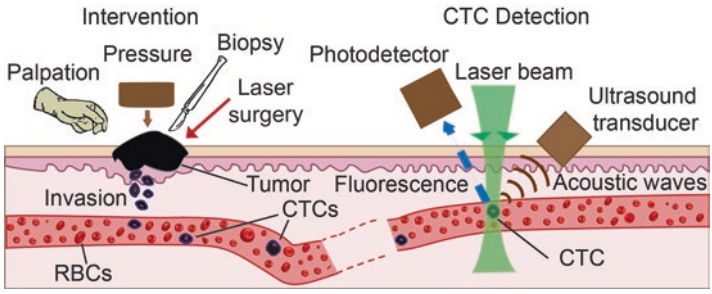

Fig. 5.1 Principle of *in vivo* flow cytometry using PA and fluorescence methods for real-time monitoring of melanoma and breast CTCs directly in the bloodstream during palpation, pressure, biopsy, and surgery. (Reproduced from Juratli et al. [22, 25])

5.4 Relationship Between Cancer Treatment and CTC Release

Using tumor-bearing mouse models, the CTC dynamic was studied during cancer treatment and afterwards. Melanoma and breast cancer cell lines inoculated in nude mice were used. The effect of biopsy and surgery on CTC dynamics was studied.

5.4.1 CTC Dynamics, and Tumor Growth in Tumor-Bearing Mice Without Interventions (Control)

Breast cancer tumor-bearing mice (n = 6) were used as control group to identify the normal rate for CTC release by the tumor. CTCs were detected by FFC and using their intrinsic fluorescence contrast (GFP expression). The average CTC count varied between 0.5 and 2 cells/min during the first 8 weeks of tumor growth, and peaked at the third and fifth weeks (Fig. 5.2). Fluctuating CTC count did not strongly correlate with tumor size in our orthotropic tumor-bearing mouse model [23].

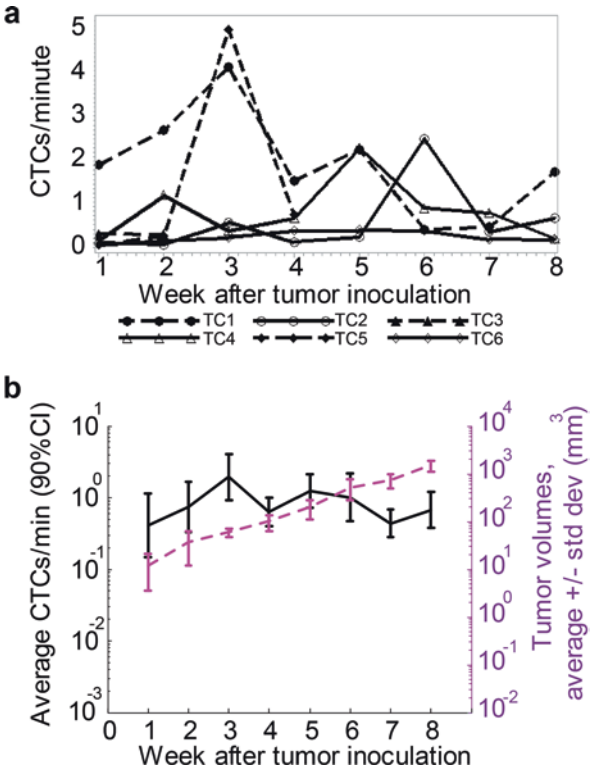

Fig. 5.2 (**a**) Profile plot of CTC detection rates (in CTCs/minute) measured weekly from six different mice inoculated with breast cancer cells (MDA-MB-LUC2-GFP) during the 8 weeks after tumor inoculation, (**b**) profile plot of the average number of CTC signals per minute and average tumor volume during the same 8 weeks. Values and error bars represent the averages and SDs of CTC counts from n = 6 mice. (Reproduced from Juratli et al. [23])

5.4.2 Tumor Biopsy-Related CTC Release

Two kinds of biopsy using two different tumor-bearing mouse models were conducted to study the effect of biopsy on CTC dynamics. Incisional biopsy in a melanoma-bearing mouse model and punch biopsy in a breast cancer-bearing mouse model were performed.

5.4.2.1 Incisional Biopsy in Melanoma-Bearing Mouse Model

Five Melanoma-bearing mice were tested using *in vivo* PAFC, relying on the intrinsic melanin in CTCs. Mice were monitored continuously for 60 min before, 15 min during, and 260 min after incisional biopsy. The baseline CTC detection rate was 1.3 cells/10 min before biopsy began. During the 15-min biopsy period, CTC rate soared to 75.1 cells/10 min, a 58-fold increase compared to baseline ($P < 0.0001$). During the first hour after the biopsy concluded, CTC rate remained high at 44.3 cells/10 min, which was 34-fold higher than the baseline ($P < 0.0001$). It decreased thereafter, but remained significantly elevated at sixfold above baseline ($P = 0.049$) during the second hour after biopsy, and at threefold above baseline ($P = 0.007$) afterwards (Fig. 5.3a–c) [22].

In two instances, we performed a second incisional biopsy 1 h after the first one. We also detected a total of 200 CTCs during the first 10 min after the second biopsy. This number was less than the first time, where we observed a total of 380 CTCs during the same period (Fig. 5.3d) [22].

5.4.2.2 Punch Biopsy in Breast Cancer-Bearing Mouse Model

A punch biopsy was conducted in six mice bearing MDA-231-MB-GFP breast cancer tumor 2 weeks after tumor inoculation. A 2.0 mm biopsy punch with a plunger system (BPP-20F 2.0 mm w/plunger, Miltex, Inc.) was used for biopsy. Cells expressing GFP were detected using FFC.

During the 8 weeks of monitoring, CTC detection rate varied from 0.2 to 1.6 cells/min (Fig. 5.4a, b). In comparison to control group (Sect. 5.4.1), average CTC rate after the biopsy was steadier (Fig. 5.4a, b). Tumor volume increased continuously throughout the experiment (Fig. 5.4b–e). The punch biopsy performed at the second week after tumor inoculation did not affect the tumor volume in five of the total of six mice. The tumor volume increased continuously during the 8 weeks after tumor inoculation. However, the punch biopsy immediately caused a significant increase in the number of CTCs at week 2. The baseline average CTC rate during 1 h before the biopsy (0.64 cells/min) was elevated to 1.17 cells/min for the 2 h after biopsy ended ($P = 0.021$; Fig. 5.4d) [23].

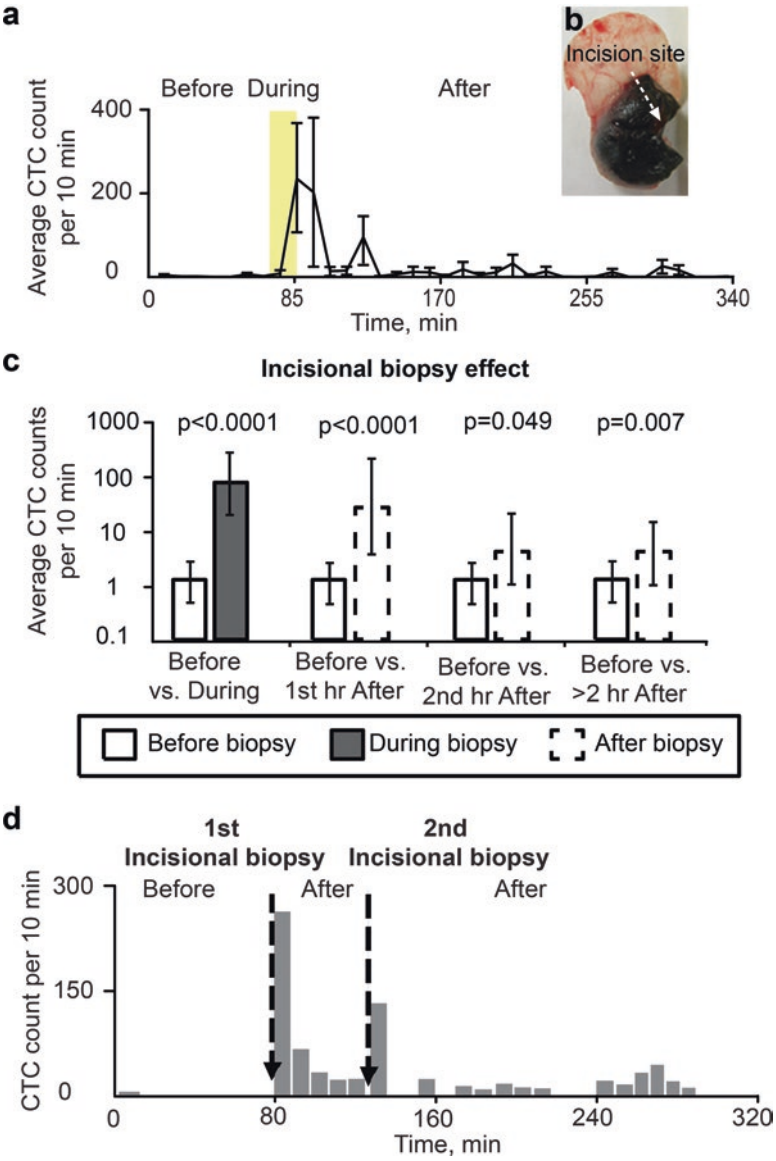

Fig. 5.3 (**a**) Histogram of average CTC counts per 10-min window for 70 min before, 15 min during (*yellow region*) and 260 min after incisional biopsy. Values and error bars represent the averages and SDs of CTC counts from n = 5 mice during each 10-min bin, (**b**) tumor after incisional biopsy, (**c**) CTC detection rates in counts per 10 min before vs. during biopsy, and before vs. after biopsy. Values (error bars) represent the estimates (90% confidence intervals) determined from mixed-models Poisson-regression analysis, (**d**) example of histogram of CTCs release before, and after two different incisional biopsies in the same mouse (B16F10-GFP) (duration of each incisional biopsy: approx. ~1 min). (Reproduced from Juratli et al. [22, 25])

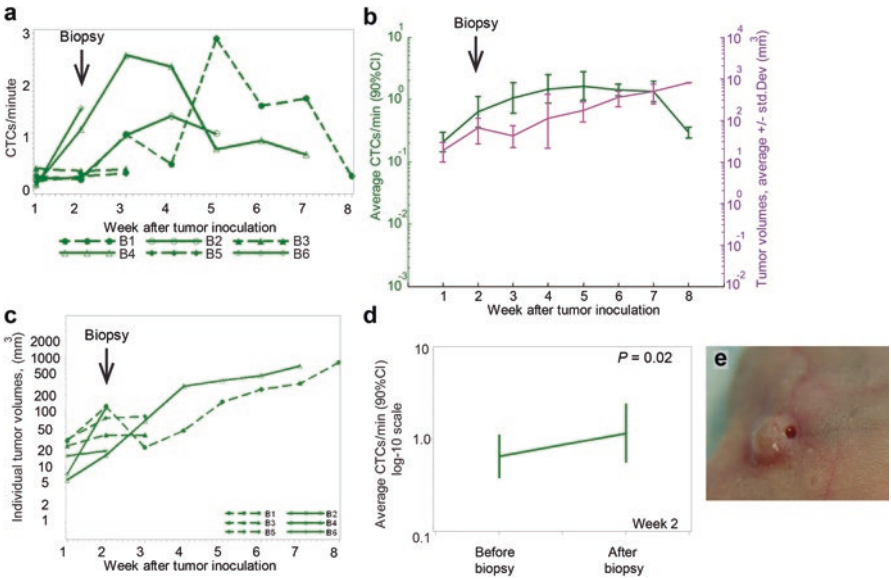

Fig. 5.4 (**a**) Profile plot of CTC detection rate number of CTCs per minute measured weekly from six mice inoculated with breast cancer cells (MDA-MB-LUC2-GFP) during the 8 weeks after tumor inoculation. Punch biopsy was performed at week 2 after tumor inoculation, (**b**) profile plot over time of the average number of CTC signals per minute and average of the tumor volume during the same 8 weeks. Values and error bars represent the averages and SDs of CTC counts from n = 6 mice. The average CTC rate per 8 weeks was calculated for five mice at week 3, three mice at week 5 and two mice at week 7, (**c**) individual tumor volumes from six mice. Punch biopsy was performed at week 2 after tumor inoculation, (**d**) profile plot of the average number of CTC signals per minute from 60 min before to 120 min after the punch biopsy, showing a 1.82-fold increase in the CTC-detection rate ($P = 0.02$), (**e**) image of the tumor after a punch biopsy. (Reproduced from Juratli et al. [23])

5.4.3 Tumor Surgery-Related CTC Release

To study the effect of surgery on CTC dynamics, complete tumor resection was conducted in melanoma-bearing mouse model and in breast cancer-bearing mouse model.

5.4.3.1 Complete Tumor Resection in Melanoma-Bearing Mouse Model

Seven mice with melanoma tumors on their right ears underwent tumor resection. PAFC was performed to enumerate CTCs in a blood vessel of the left ear, before and after the tumor resection. During the 50 min of baseline recording prior to tumor resection, a total of 35 CTCs were detected among the 7 mice (an average of 1 CTC/10 min). In contrast, no increase in CTC rate was observed during

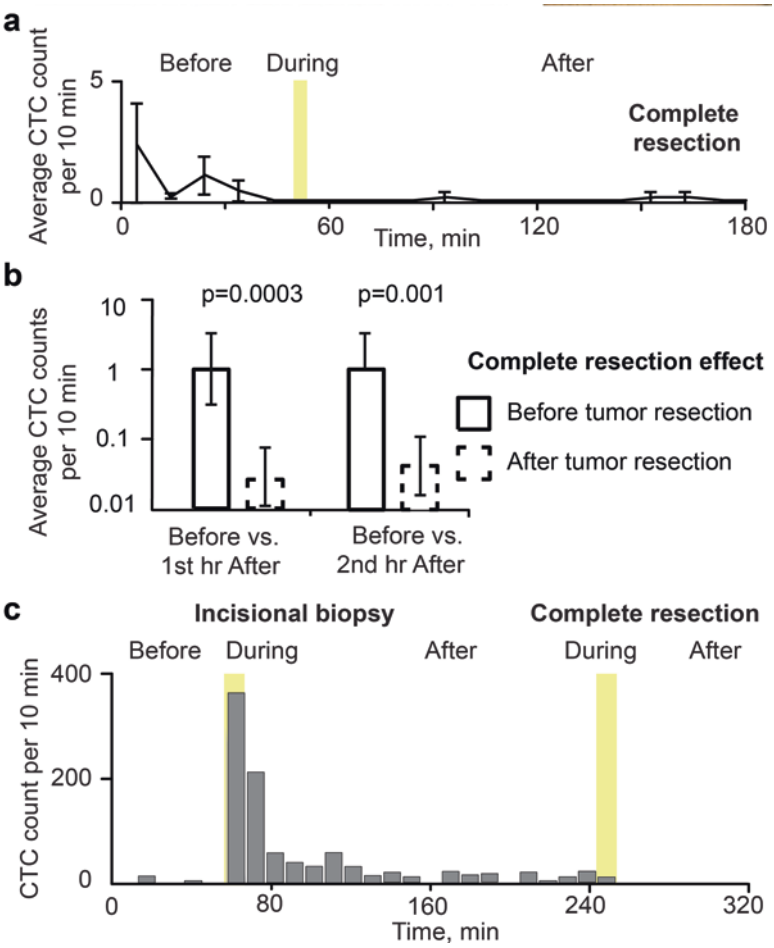

Fig. 5.5 (**a**) Histogram of average CTC signal number per 10 min from before, 5 min during (*yellow region*) and after complete tumor resection. Values and error bars represent the averages and SDs of CTC counts from n = 7 mice during each 10-min bin, (**b**) CTC detection rates in counts per 10 min before vs. the first hour and second hour after surgery. During complete resection, no CTCs were detected. Values (error bars) represent the estimates (90% confidence intervals) determined from mixed-models Poisson-regression analysis, (**c**) Example of histogram of CTCs release before, and after incisional biopsy (duration of incisional biopsy: approx. 10 min), and tumor complete resection with tumor manipulation (duration of complete tumor resection: approx. 10 min) (B16F10-GFP). (Reproduced from Juratli et al. [22, 25])

surgery, and only one CTC was detected during the first hour after resection (0.023 CTCs/10 min; $P = 0.0002$), and only two CTCs were detected during the second hour after resection (0.047 CTCs/10 min; $P = 0.0005$) among the seven mice. Two to three hours after tumor resection, no CTCs were detected in any mouse (Fig. 5.5a, b) [22].

5.4.3.2 Incisional Biopsy Followed by Complete Tumor Resection in Melanoma-Bearing Mouse Model

In two cases, a complete tumor resection was conducted 2 h after the incisional biopsy. The tumor (B16F10-GFP) was squeezed with a surgical instrument during resection. Twenty CTCs were observed during 10 min of resection time and no CTCs were detected up to 1 h after the complete resection was completed (Fig. 5.5c) [22].

5.4.3.3 Complete Tumor Resection in Breast Cancer-Bearing Mouse Model

On a group of six mice, tumor resection was conducted 2 weeks after inoculation of MDA-MB-231 breast cancer cells in the mammary gland. In five of them, tumor-free margins were achieved and there was no residual tumor left, which was confirmed by histology exams performed on the resected tumors.

A dramatic decrease in the number of CTCs was observed compared to the control group (Sect. 5.4.1); from 0.1 CTCs/min at second week to ~0.01 CTCs/min at weeks three-to-eight (Fig. 5.6a, b). However, CTC recurrence in small numbers was detected during the 5 weeks following surgery (Fig. 5.6a, b).

No tumor visibly re-grew in any of the mice during the 6 weeks after tumor resection (Fig. 5.6b). A short-term effect of complete tumor resection was also profound. While a total of 28 CTCs were detected during 1 h before resection (0.08 CTCs/min, $n = 6$), no CTCs were observed during and for 2 h after the resection ($P = 0.03$) (Fig. 5.6d) [23].

In one of the mice (S5), histology exam of the resected tumor revealed a positive tumor margin (Fig. 5.5a). The CTC rate for this mouse was the highest in the group for 6 weeks after the surgery, and the maximum CTC rate was observed 2 weeks after the surgery [23].

5.4.4 Novel Techniques for Identification of Released CTC

The quantification of CTC release triggered by manipulation is complicated by the presence of CTCs that were shed from tumor sometime before the manipulation. This requires the use of complex statistical methods to confirm the release of CTCs as the result of manipulations. Novel tools for labeling tumor cells bring a promise of simple identification of newly released CTCs among already circulating ones. Both photoswitchable fluorescent proteins (e.g. Dendra2 [32, 33]) as contrast agents for fluorescence flow cytometry and photoswitchable nanoparticles (NPs) for PA detection have been proposed to identify manipulation-released CTCs [32, 34].

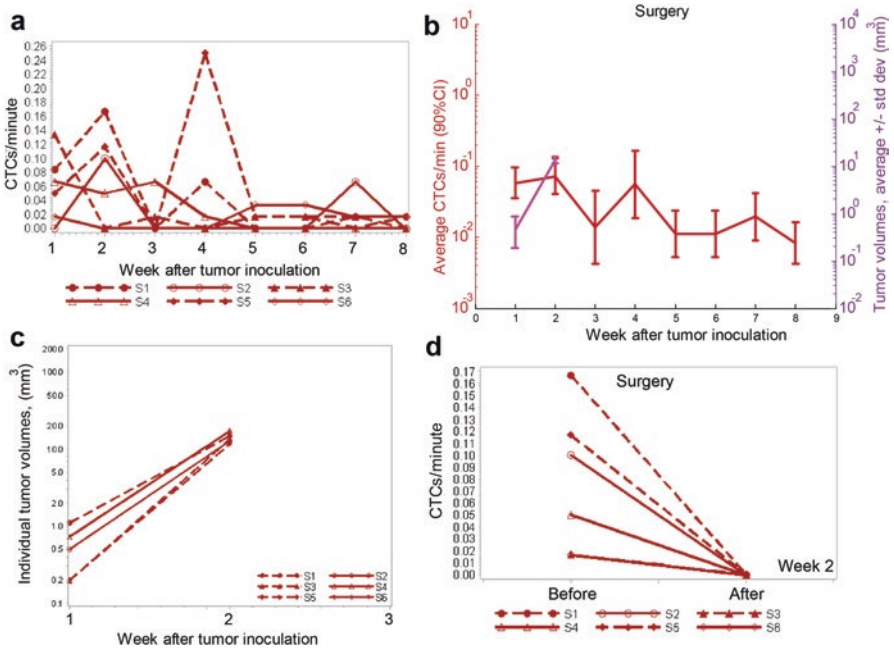

Fig. 5.6 (**a**) Profile plot of CTC detection rates (in CTCs/minute) measured weekly from six mice inoculated with breast cancer cells (MDA-MB-LUC2-GFP). Surgery was conducted at Week 2 after tumor inoculation, (**b**) profile plot of the average number of CTC signals per minute and average tumor volume during 8 weeks from n = 5 mice after excluding the mouse which received partial tumor resection. Values and error bars represent the averages and SDs of CTC counts from n = 5 mice, (**c**) individual tumor volumes from six mice. Surgery was performed at week 2 after tumor inoculation, (**d**) profile plot of the average number of CTC signals per minute from 60 min before and 120 min after the surgery. (Reproduced from Juratli et al. [23])

5.4.4.1 Photoswitchable Fluorescent Proteins

Photoswitchable fluorescent protein Dendra2 normally fluoresces in green, however, it can be irreversibly switched into red color using 405 nm laser [35]. A photoswitchable fluorescence cytometry (PFC) for noninvasive enumeration of red and green cells, as well as switching of primary tumor cells and of individual CTCs in blood flow was developed [34]. The principles of CTCs identification using photoswitchable proteins were demonstrated using a mouse ear model of metastatic carcinoma (MTLn3 adenocarcinoma cells expressing Dendra2 protein). Thin ear structures and isolated tumor location allow successful photoswitching of all the primary tumor cells, and noninvasive fluorescence imaging to control switching efficacy laser. Dual color (green and red) monitoring of CTCs released from the primary tumor has indicated that only green cells are released from the primary tumor, and possibly, from already established metastases. However, after the primary tumor was completely converted into "red" state (i.e. Dendra2 protein in all the primary tumor cells was switched to red color), it was able to detect both green

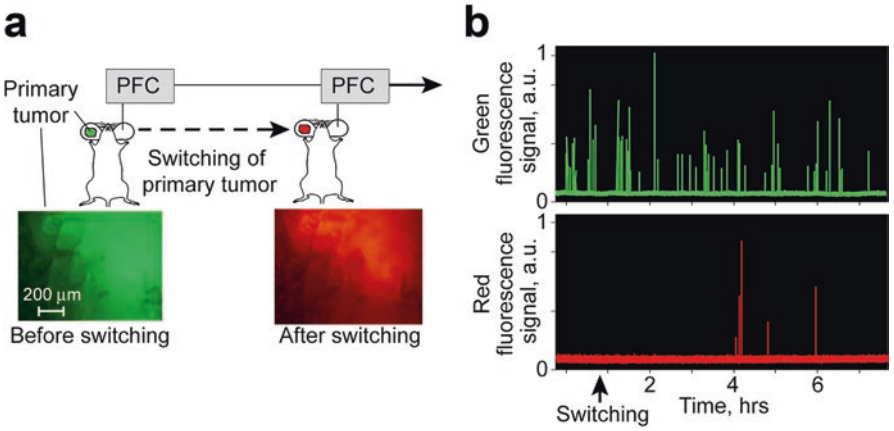

Fig. 5.7 (**a**) Concept of switching the primary tumor cells from *green* to *red* state; (**b**) dual color detection of circulating cells in peripheral blood flow (56 µm diameter ear vein) after photoswitching of the primary tumor. *Green signals* correspond to non-switched CTCs shed into flow before switching of the primary tumor, *red signals* correspond to photoswitched cells released after conversion. (Reproduced from Nedosekin et al. [34])

(old CTCs) and red (recently released CTCs) in circulation. Without manipulation, first red CTCs were detected ~180 min after switching indicating that it was spontaneous shedding [25]. Moreover, high irregularity in the dynamics of new CTCs release was observed. The same model can be extended to study release of CTCs from metastases (non-switched metastases will keep producing green CTCs), given that primary tumor may shed only red cells and all the old green CTCs will eventually leave the circulation (Fig. 5.7) [34].

5.5 Discussion and Conclusion

The major cause of cancer-associated mortality is tumor metastasis. CTCs which during successful dissemination invade the surrounding primary tumor tissue, intravasate into blood, lymph and cerebrospinal fluid and could form metastases [36, 37]. Therefore, one of the most promising approaches to prevent metastatic disease is the early detection of CTCs and to avoid interventions which could lead to an increase in CTC rate.

This work was designed with the overall goal to determine the dynamic fluctuation of CTCs during medical interventions using breast cancer and melanoma-bearing mouse models. The PAFC and FFC allowed us to monitor the CTC dynamics noninvasively and in real-time in physiologically and clinically relevant conditions. The well-established murine xenograft mouse model was used in these studies. This model has several advantages to determine CTC dynamics during tumor growth and medical interventions because of (1) the use of actual human tumor tissue; (2)

results could be obtained during the few weeks from tumor inoculation; (3) the organ environment in which the tumor growth could be reproduced [38]. However, the immunological deficit is a disadvantage for using this model. For the first time, it was possible to monitor the same mouse frequently up to 8 weeks after tumor inoculation and to study the change in CTC rate during tumor biopsy and surgery.

This work aimed to determine the short term of the CTC dynamic fluctuation due to different diagnostic and treatment procedures. Here experimental evidence that incisional biopsy increased the CTC rate up to 60-fold during the procedures in a melanoma-bearing mouse model was presented. In contrast, complete tumor resection led to decrease of CTC rate and in some cases to disappearance shortly afterwards. One of the most interesting findings in this work could be the discrepancy between the effects of incisional biopsy versus excisional biopsy on CTC count. This analysis is very timely and relevant, as tumor manipulation is a key point of interest for the practicing surgeon. To study the CTC dynamics for long-term after procedures, breast cancer-bearing mice were used. In this study, marked increase in CTC rate was determined during the punch biopsy. In the melanoma-bearing mouse model, however, a higher level of CTC rate was monitored shortly afterwards. Different outcome was observed after complete tumor resection by disappearance of the CTCs. However, in some cases low level of CTC re-elevation during 6 weeks after the procedure was observed in the breast cancer-bearing mice.

The results of this work provide further support that tumor manipulation, by offering greater opportunity for tumor cell invasion into the circulation, could result in shedding of malignant cells into the circulatory system and possibly in turn will affect the prognosis by increasing the risk of metastasis [39]. However, these data must be interpreted with caution because of the immunological deficit of the tumor bearing-mouse models used and because of the CTCs, which are rare and not all may be clinically relevant in the human body [37]. Thus, further research is needed to examine CTC dynamic in human *in vivo* during tumor growth and medical interventions.

References

1. Galanzha EI, Zharov VP (2013) Circulating tumor cell detection and capture by photoacoustic flow cytometry in vivo and ex vivo. Cancers (Basel) 5:1691–1738
2. Pantel K, Brakenhoff RH, Brandt B (2008) Detection, clinical relevance and specific biological properties of disseminating tumour cells. Nat Rev Cancer 8:329–340
3. Kaiser J (2010) Medicine. Cancer's circulation problem. Science 327:1072–1074
4. Yu M, Bardia A, Wittner BS, Stott SL, Smas ME et al (2013) Circulating breast tumor cells exhibit dynamic changes in epithelial and mesenchymal composition. Science 339:580–584
5. Yu M, Stott S, Toner M, Maheswaran S, Haber DA (2011) Circulating tumor cells: approaches to isolation and characterization. J Cell Biol 192:373–382
6. Weitz J, Kienle P, Lacroix J, Willeke F, Benner A et al (1998) Dissemination of tumor cells in patients undergoing surgery for colorectal cancer. Clin Cancer Res 4:343–348
7. Louha M, Nicolet J, Zylberberg H, Sabile A, Vons C et al (1999) Liver resection and needle liver biopsy cause hematogenous dissemination of liver cells. Hepatology 29:879–882

8. Loughran CF, Keeling CR (2011) Seeding of tumour cells following breast biopsy: a literature review. Br J Radiol 84:869–874
9. Katharina P (2011) Tumor cell seeding during surgery-possible contribution to metastasis formations. Cancers (Basel) 3:2540–2553
10. Patel H, Le Marer N, Wharton RQ, Khan ZA, Araia R et al (2002) Clearance of circulating tumor cells after excision of primary colorectal cancer. Ann Surg 235:226–231
11. Fan ZC, Yan J, Liu GD, Tan XY, Weng XF et al (2012) Real-time monitoring of rare circulating hepatocellular carcinoma cells in an orthotopic model by in vivo flow cytometry assesses resection on metastasis. Cancer Res 72:2683–2691
12. Wind J, Tuynman JB, Tibbe AG, Swennenhuis JF, Richel DJ et al (2009) Circulating tumour cells during laparoscopic and open surgery for primary colonic cancer in portal and peripheral blood. Eur J Surg Oncol 35:942–950
13. He W, Wang H, Hartmann LC, Cheng JX, Low PS (2007) In vivo quantitation of rare circulating tumor cells by multiphoton intravital flow cytometry. Proc Natl Acad Sci U S A 104:11760–11765
14. Riethdorf S, Fritsche H, Muller V, Rau T, Schindlbeck C et al (2007) Detection of circulating tumor cells in peripheral blood of patients with metastatic breast cancer: a validation study of the CellSearch system. Clin Cancer Res 13:920–928
15. Bednarz-Knoll N, Alix-Panabieres C, Pantel K (2011) Clinical relevance and biology of circulating tumor cells. Breast Cancer Res 13:228
16. Wei X, Sipkins DA, Pitsillides CM, Novak J, Georgakoudi I et al (2005) Real-time detection of circulating apoptotic cells by in vivo flow cytometry. Mol Imaging 4:415–416
17. Kusukawa J, Suefuji Y, Ryu F, Noguchi R, Iwamoto O et al (2000) Dissemination of cancer cells into circulation occurs by incisional biopsy of oral squamous cell carcinoma. J Oral Pathol Med 29:303–307
18. Hayashi K, Jiang P, Yamauchi K, Yamamoto N, Tsuchiya H et al (2007) Real-time imaging of tumor-cell shedding and trafficking in lymphatic channels. Cancer Res 67:8223–8228
19. Novak J, Georgakoudi I, Wei X, Prossin A, Lin CP (2004) In vivo flow cytometer for real- time detection and quantification of circulating cells. Opt Lett 29:77–79
20. Georgakoudi I, Solban N, Novak J, Rice WL, Wei X et al (2004) In vivo flow cytometry: a new method for enumerating circulating cancer cells. Cancer Res 64:5044–5047
21. Nedosekin DA, Sarimollaoglu M, Galanzha EI, Sawant R, Torchilin VP et al (2013) Synergy of photoacoustic and fluorescence flow cytometry of circulating cells with negative and positive contrasts. J Biophotonics 6:425–434
22. Juratli MA, Sarimollaoglu M, Siegel ER, Nedosekin DA, Galanzha EI et al (2014) Real-time monitoring of circulating tumor cell release during tumor manipulation using in vivo photoacoustic and fluorescent flow cytometry. Head Neck 36:1207–1215
23. Juratli MA, Siegel ER, Nedosekin DA, Sarimollaoglu M, Jamshidi-Parsian A et al (2015) In vivo long-term monitoring of circulating tumor cells fluctuation during medical interventions. PLoS One 10:e0137613
24. Zharov VP, Galanzha EI, Tuchin VV (2005) Integrated photothermal flow cytometry in vivo. J Biomed Opt 10:051502
25. Juratli MA, Sarimollaoglu M, Nedosekin DA, Melerzanov AV, Zharov VP et al (2014) Dynamic fluctuation of circulating tumor cells during cancer progression. Cancers (Basel) 6:128–142
26. Menyaev YA, Nedosekin DA, Sarimollaoglu M, Juratli MA, Galanzha EI et al (2013) Optical clearing in photoacoustic flow cytometry. Biomed Opt Express 4:3030–3041
27. Sarimollaoglu M, Nedosekin DA, Menyaev YA, Juratli MA, Zharov VP (2014) Nonlinear photoacoustic signal amplification from single targets in absorption background. Photoacoustics 2:1–11
28. Nedosekin DA, Juratli MA, Sarimollaoglu M, Moore CL, Rusch NJ et al (2013) Photoacoustic and photothermal detection of circulating tumor cells, bacteria and nanoparticles in cerebrospinal fluid in vivo and ex vivo. J Biophotonics 6:523–533

29. Galanzha EI, Kim JW, Zharov VP (2009) Nanotechnology-based molecular photoacoustic and photothermal flow cytometry platform for in-vivo detection and killing of circulating cancer stem cells. J Biophotonics 2:725–735
30. Galanzha EI, Shashkov EV, Spring PM, Suen JY, Zharov VP (2009) In vivo, noninvasive, label-free detection and eradication of circulating metastatic melanoma cells using two- color photoacoustic flow cytometry with a diode laser. Cancer Res 69:7926–7934
31. Galanzha EI, Zharov VP (2012) Photoacoustic flow cytometry. Methods 57:280–296
32. Galanzha EI, Nedosekin DA, Sarimollaoglu M, Orza AI, Biris AS et al (2015) Photoacoustic and photothermal cytometry using photoswitchable proteins and nanoparticles with ultrasharp resonances. J Biophotonics 8:81–93
33. Yao J, Kaberniuk AA, Li L, Shcherbakova DM, Zhang R et al (2016) Multiscale photoacoustic tomography using reversibly switchable bacterial phytochrome as a near-infrared photochromic probe. Nat Methods 13:67–73
34. Nedosekin DA, Verkhusha VV, Melerzanov AV, Zharov VP, Galanzha EI (2014) In vivo photoswitchable flow cytometry for direct tracking of single circulating tumor cells. Chem Biol 21:792–801
35. Kedrin D, Gligorijevic B, Wyckoff J, Verkhusha VV, Condeelis J et al (2008) Intravital imaging of metastatic behavior through a mammary imaging window. Nat Methods 5:1019–1021
36. Pantel K, Alix-Panabieres C (2012) Detection methods of circulating tumor cells. J Thorac Dis 4:446–447
37. Plaks V, Koopman CD, Werb Z (2013) Cancer. Circulating tumor cells. Science 341: 1186–1188.
38. Richmond A, Su Y (2008) Mouse xenograft models vs GEM models for human cancer therapeutics. Dis Model Mech 1:78–82
39. Davies MM, Mathur P, Carnochan P, Saini S, Allen-Mersh TG (2002) Effect of manipulation of primary tumour vascularity on metastasis in an adenocarcinoma model. Br J Cancer 86:123–129